

Multi-step multi-beam laser interference patterning of three-dimensional photonic lattices

Satoru Shoji^a, Remo Proietti Zaccaria^{a,b}, Hong-Bo Sun^{a,c}, and Satoshi Kawata^{a,d}

^aDepartment of Applied Physics, Osaka University, Yamadaoka 2-1, Suita, Osaka 565-0871, Japan

^bMagna Graecia University, BIONEM laboratory, Campus Germaneto, Viale Europa, 88100 Catanzaro, Italy

^cState Key Laboratory on Integrated Optoelectronics, College of Electrical Science and Engineering, Jilin University, China

^dNanophotonics laboratory, RIKEN, Hirosawa, Wako, Saitama 351-0198, Japan

shoji@ap.eng.osaka-u.ac.jp

<http://lasie.ep.eng.osaka-u.ac.jp/>

Abstract: We present laser interference patterning of three-dimensional photonic lattice structures with three-step three-beam irradiation. In contrast to one-step four-beam interference patterning, the proposed method makes it possible to continuously tune the lattice constant and the photonic band gap without distortion of the lattice shape. We analytically show that all fourteen Bravais lattices are possible to be produced by choosing proper incident vectors of laser beams. A simple routine to seek the geometrical configuration of the incident beams for producing arbitrary Bravais lattices is shown. Furthermore, We experimentally demonstrate the fabrication of three-dimensional photonic lattices in the photoresist SU-8. Significant photonic band gap effects have been observed from the well-defined photonic lattices.

© 2006 Optical Society of America

OCIS codes: (220.4000) Microstructure fabrication, (220.4610) Optical fabrication, (090.2880) Holographic interferometry, (230.0250) Optoelectronics.

References and links

1. J. Joannopoulos, P. R. Villeneuve, and S. Fan, "Photonic crystals: putting a new twist on light," *Nature (London)* **386**, 143–149 (1997).
2. L. Z. Cai, X. L. Yang, and Y. R. Wang, "All fourteen Bravais lattices can be formed by interference of four noncoplanar beams," *Opt. Lett.* **27**, 900–902 (2002).
3. M. Campbell, D. N. Sharp, M. T. Harrison, R. G. Denning, and A. J. Turberfield, "Fabrication of photonic crystals for the visible spectrum by holographic lithography," *Nature (London)* **404**, 53–56 (2000).
4. S. Shoji and S. Kawata, "Photofabrication of three-dimensional photonic crystals by multibeam laser interference into a photopolymerizable resin," *Appl. Phys. Lett.* **76**, 2668–2670 (2000).
5. D. N. Sharp, A. J. Turberfield, and R. G. Denning, "Holographic photonic crystals with diamond symmetry," *Phys. Rev. B* **68**, 205102 (2003).
6. S. Shoji, H.-B. Sun, and S. Kawata, "Photofabrication of wood-pile three-dimensional photonic crystals using four-beam laser interference," *Appl. Phys. Lett.* **83**, 608–610 (2003).
7. G. J. Schneider, E. D. Wetzel, J. A. Murakowski, and D. W. Prather, "Fabrication of three-dimensional Yablonovite photonic crystals by multiple-exposure UV interference lithography," *Proc. SPIE* **5720**, 9 (2005).

8. S. Shoji, H.-B. Sun, and S. Kawata, "Multi-Beam Interference Laser Fabrication of an Inverse Structure of Yablonovite Photonic Crystal," Technical Digest of International Symposium on Photonic and Electromagnetic Crystal Structures V (PECS-V), 34 (2004).
9. L. Z. Cai, X. L. Yang, and Y. R. Wang, "Formation of a microfiber bundle by interference of three noncoplanar beams," Opt. Lett. **26**, 1858–1860 (2001).
10. L. Yuan, G. P. Wang, and X. Huang, "Arrangements of four beams for any Bravais lattice," Opt. Lett. **28**, 1769–1771 (2003).
11. Yu. V. Miklyaev, D. C. Meisel, A. Blanco, G. von Freymann, K. Busch, W. Koch, C. Enkrich, M. Deubel, and M. Wegener, "Three-dimensional face-centered-cubic photonic crystal templates by laser holography: fabrication, optical characterization, and band-structure calculations," Appl. Phys. Lett. **82**, 1284 (2003).
12. E. Yablonovitch, T. J. Gmitter, and K. M. Leung, "Photonic Band Structure: The Face-Centered-Cubic Case Employing Nonspherical Atoms," Phys. Rev. Lett. **67**, 2295–2298 (1991).

1. Introduction

Photonic crystals are expected as the novel nanophotonic structures which enable us the ultimate manipulation of photons[1]. Laser interference fabrication is a promising method for three-dimensional(3D) photonic crystals, because of not only the simplicity of the fabrication process, apparatus, or the ability to produce a large number of periods in three dimensions at optical wavelength, but also its flexibility for the lattice design. According to the number of laser beams and their configuration (ie. the incident angles and the phase), various symmetries of 3D lattices can be produced. Analytical investigation shows that all fourteen Bravais lattices can be produced by interference of four noncoplanar laser beams[2], and experimentally a variety of structures such as face-centered and body-centered cubic (fcc, bcc)[3], simple hexagonal lattice[4], diamond lattice[5], wood-pile lattice[6], and Yablonovite lattice[7, 8] were demonstrated with photosensitive polymers. However, still there is a difficulty to choose the lattice symmetry and the lattice constant independently in most types of interference fabrication methods. Because the configuration of laser beams determines both the symmetry of the lattice and the lattice constant at the same time, and in most cases a freedom of the wavelength of laser beams is restricted by photosensitivity of materials, and by the availability of lasers.

We have proposed multi-step exposure for laser interference fabrication[4, 6]. We produced interference patterns of low-dimensional periodicity rather than 3D periodicity, and then, performed multi-time exposure from different directions into materials to create a 3D lattice structure. This method makes it possible to freely choose the lattice constant, independent on the lattice symmetry or the shape of the lattice element. In this paper, we discuss three-step and three-beam interference exposure and fabrication of scaffold type 3D photonic crystal structures of three intersecting rod arrays. A simple routine to seek the geometrical configuration of the incident beams for all fourteen Bravais lattices is shown.

2. Theoretical

First, we consider the primitive lattice; a simple-cubic lattice, which consists of a combination of rod-arrays traveling in three directions, $(0, 0, 1)$, $(0, 1, 0)$, and $(1, 0, 0)$. Each rod-array is in the order of square lattice. According to a previous report by Cai[9], periodic rod-arrays with any types of 2D Bravais lattices arrangement can be formed by three noncoplanar beams. A square lattice rod-array is one of them. For example, for the rod-array in the direction $(0, 0, 1)$ one candidate pair of wave vectors of laser beams can be chosen as follows,

$$\mathbf{k}_{11} = \left(\frac{k \sin \theta}{\sqrt{2}}, \frac{k \sin \theta}{\sqrt{2}}, k \cos \theta \right),$$

$$\mathbf{k}_{12} = \left(-\frac{k \sin \theta}{\sqrt{2}}, \frac{k \sin \theta}{\sqrt{2}}, k \cos \theta \right),$$

$$\mathbf{k}_{13} = \left(\frac{k \sin \theta}{\sqrt{2}}, -\frac{k \sin \theta}{\sqrt{2}}, k \cos \theta \right). \quad (1)$$

where, k_{ij} is the wave vectors of j th beams in i th irradiation, k is the wave number $k = |\mathbf{k}_{ij}| = 2\pi/\lambda$, and θ is the inclination angle of the laser beams from the plane normal to rods. In the same way, other two groups of three laser beams for the rest two rod arrays in $(0,1,0)$ and $(1,0,0)$ can be easily found by rotation operation as; $\mathbf{k}_{21} = (k \sin \theta/\sqrt{2}, k \cos \theta, k \sin \theta/\sqrt{2})$, $\mathbf{k}_{22} = (-k \sin \theta/\sqrt{2}, k \cos \theta, k \sin \theta/\sqrt{2})$, $\mathbf{k}_{23} = (k \sin \theta/\sqrt{2}, k \cos \theta, -k \sin \theta/\sqrt{2})$, and $\mathbf{k}_{31} = (k \cos \theta, k \sin \theta/\sqrt{2}, k \sin \theta/\sqrt{2})$, $\mathbf{k}_{32} = (k \cos \theta, -k \sin \theta/\sqrt{2}, k \sin \theta/\sqrt{2})$, $\mathbf{k}_{33} = (k \cos \theta, k \sin \theta/\sqrt{2}, -k \sin \theta/\sqrt{2})$.

The light pattern produced by three-step three-beam laser interference can be given as,

$$I(\mathbf{r}) = \sum_{i=1}^3 \sum_{0 \leq j < j' \leq 3} \mathbf{E}_{ij} \mathbf{E}_{ij'} \exp[i\{(\mathbf{k}_{ij} - \mathbf{k}_{ij'})\mathbf{r} + \phi_{ij} - \phi_{ij'}\}]. \quad (2)$$

where \mathbf{E}_{ij} , ϕ_{ij} are amplitude and phase delay of the electric field, and the maximum light intensity is at $(\mathbf{k}_{ij} - \mathbf{k}_{ij'})\mathbf{r} = 2n\pi$ (n is an integer number). Specifically, the differences $\mathbf{k}_{ij} - \mathbf{k}_{ij'}$ determines the reciprocal lattice vectors of the resultant light pattern. If all the laser beams have the same intensity and phase delay, the rod arrays intersect each other on the points, which are ordered in three-dimensional simple square lattice. Fig. 1 shows the calculated light intensity distribution formed by three-step irradiation three-beam laser interference with the aforementioned beam geometries, which gives scaffold shaped simple-cubic lattice. The lattice constant (i.e., the distance between the nearest neighbor rods) $d = \lambda/\sqrt{2}\sin \theta$ is freely chosen by θ without distortion of the lattice element and lattice symmetry.

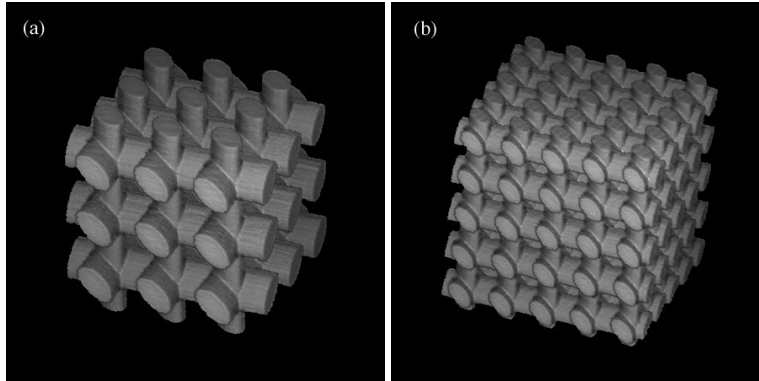


Fig. 1. Three-dimensional simple-cubic lattices created by three-step three-beam laser interference. In the calculation, the wavelength of laser light is 355 nm, the size of calculation space is 5 μm . The inclination angle of the laser beams θ is (a)10° and (b)15°.

Next, other arbitrary types of 3D Bravais lattices are considered. For all Bravais lattices, including the simple-cubic lattice, lattice points (i.e., position of the atoms in solid crystals) can be described by three primitive translation vectors as

$$\mathbf{R} = u_1 \mathbf{a}_1 + u_2 \mathbf{a}_2 + u_3 \mathbf{a}_3. \quad (3)$$

where u_i is integer number and \mathbf{a}_i is the primitive translation vector which defines the lattice type. The most simple lattice is simple-cubic, in which three primitive translation vectors are given as $\mathbf{a}_{01} = (a, 0, 0)$, $\mathbf{a}_{02} = (0, a, 0)$, $\mathbf{a}_{03} = (0, 0, a)$, where a is the lattice constant. Since

in all kinds of Bravais lattices the position vectors of lattice points are expressed by linear combination of three translation components, any other types of Bravais lattice are expressed by the linear transformation of simple-cubic lattice. Namely, the operator matrix for the linear transformation can be defined as,

$$\Delta = \begin{pmatrix} \delta_{1x} & \delta_{2x} & \delta_{3x} \\ \delta_{1y} & \delta_{2y} & \delta_{3y} \\ \delta_{1z} & \delta_{2z} & \delta_{3z} \end{pmatrix}. \quad (4)$$

and,

$$\begin{aligned} \mathbf{A} &= \Delta \cdot \mathbf{A}_0 \\ &= \begin{pmatrix} \delta_{1x} & \delta_{2x} & \delta_{3x} \\ \delta_{1y} & \delta_{2y} & \delta_{3y} \\ \delta_{1z} & \delta_{2z} & \delta_{3z} \end{pmatrix} \begin{pmatrix} a & 0 & 0 \\ 0 & a & 0 \\ 0 & 0 & a \end{pmatrix}. \end{aligned} \quad (5)$$

where, \mathbf{A} and \mathbf{A}_0 are matrices of three translation vectors for the desired lattice and simple-cubic lattice, respectively. As one example, now we discuss about body-centered cubic (bcc) lattice. The primitive translation vectors for bcc lattice are $(a/2, a/2, -a/2)$, $(a/2, -a/2, a/2)$, and $(-a/2, a/2, a/2)$. Therefore, from equation (5) the operator matrix Δ is given as follows,

$$\Delta_{bcc} = \begin{pmatrix} 1/2 & 1/2 & -1/2 \\ 1/2 & -1/2 & 1/2 \\ -1/2 & 1/2 & 1/2 \end{pmatrix}. \quad (6)$$

As mentioned above in Eq. (2), as well as discussions in the previous reports[2, 10], the wavevectors of laser beams give reciprocal lattice translation vectors. In order to solve the wavevectors of laser beams representing the desired lattice, primitive nine wavevectors creating a simple-cubic lattice are transformed by linear transformation with reciprocal matrix of Δ ,

$$\mathbf{k}'_{ij} = \Delta^{-1} \cdot \mathbf{k}_{ij}. \quad (7)$$

With the given matrix, three pairs of three wavevectors for producing a bcc lattice are calculated from the linear transformation of nine laser wavevectors for a simple-cubic lattice.

$$\Delta_{bcc}^{-1} = \begin{pmatrix} 1 & 1 & 0 \\ 1 & 0 & 1 \\ 0 & 1 & 1 \end{pmatrix}. \quad (8)$$

and then,

$$\begin{aligned} \mathbf{k}_{11} &= \left(\frac{2k}{\sqrt{2}} \sin \theta, \frac{k}{\sqrt{2}} (\sin \theta + \sqrt{2} \cos \theta), \frac{k}{\sqrt{2}} (\sin \theta + \sqrt{2} \cos \theta) \right), \\ \mathbf{k}_{12} &= \left(0, \frac{k}{\sqrt{2}} (-\sin \theta + \sqrt{2} \cos \theta), \frac{k}{\sqrt{2}} (\sin \theta + \sqrt{2} \cos \theta) \right), \\ \mathbf{k}_{13} &= \left(0, \frac{k}{\sqrt{2}} (\sin \theta + \sqrt{2} \cos \theta), \frac{k}{\sqrt{2}} (-\sin \theta + \sqrt{2} \cos \theta) \right), \\ \mathbf{k}_{21} &= \left(\frac{k}{\sqrt{2}} (\sin \theta + \sqrt{2} \cos \theta), \frac{2k}{\sqrt{2}} \sin \theta, \frac{k}{\sqrt{2}} (\sin \theta + \sqrt{2} \cos \theta) \right), \\ \mathbf{k}_{22} &= \left(\frac{k}{\sqrt{2}} (-\sin \theta + \sqrt{2} \cos \theta), 0, \frac{k}{\sqrt{2}} (\sin \theta + \sqrt{2} \cos \theta) \right), \end{aligned}$$

$$\begin{aligned}
\mathbf{k}_{23} &= \left(\frac{k}{\sqrt{2}}(\sin \theta + \sqrt{2} \cos \theta), 0, \frac{k}{\sqrt{2}}(-\sin \theta + \sqrt{2} \cos \theta) \right), \\
\mathbf{k}_{31} &= \left(\frac{k}{\sqrt{2}}(\sin \theta + \sqrt{2} \cos \theta), \frac{k}{\sqrt{2}}(\sin \theta + \sqrt{2} \cos \theta), \frac{2k}{\sqrt{2}} \sin \theta \right), \\
\mathbf{k}_{32} &= \left(\frac{k}{\sqrt{2}}(-\sin \theta + \sqrt{2} \cos \theta), \frac{k}{\sqrt{2}}(\sin \theta + \sqrt{2} \cos \theta), 0 \right), \\
\mathbf{k}_{33} &= \left(\frac{k}{\sqrt{2}}(\sin \theta + \sqrt{2} \cos \theta), \frac{k}{\sqrt{2}}(-\sin \theta + \sqrt{2} \cos \theta), 0 \right). \tag{9}
\end{aligned}$$

Fig. 2(a) shows the result produced by these lasers. In the same way, any other kinds of Bravais lattices are produced from the analysis of primitive translation vectors systematically. Fig. 2(b) is in the case of a face-centered cubic(fcc) lattice, which represents an reverse structure of Yablonovite lattice[12].

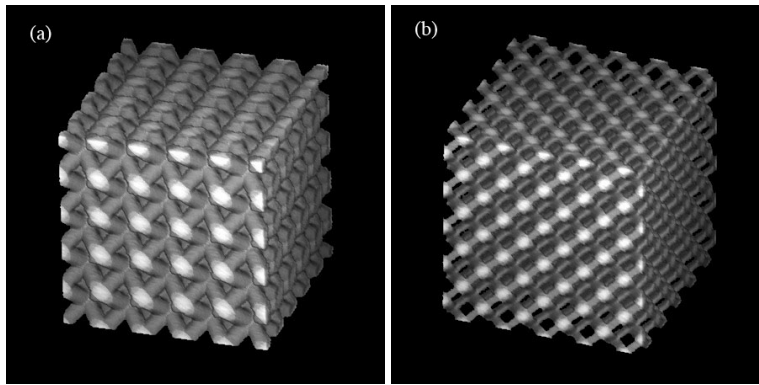


Fig. 2. Three dimensional light pattern created by three-step three-beam laser interference. (a)body-centered cubic(bcc) lattice and (b)face-centered cubic(fcc) lattice. The initial wavevectors of laser beams before linear transformation is the same as those for Fig. 1(b). The wavelength of laser light is 355 nm, the size of calculation space is 5 μm .

3. Experimental demonstration

We experimentally demonstrate three-step three-beam laser interference patterning of scaffold type 3D photonic lattices. We chose a fcc lattice for demonstration. Fig. 3 shows the optical setup. A third harmonic light of Q-switched Nd:YVO4 laser(BL6S-355Q, Spectra-Physics Inc.) was split into three beams with two beam-splitter cubes. The three beams traveled through each optical path, and were reflected by three mirrors into a photoresist film. The photoresist film was fixed on a stage which could be rotated and tilted so that the incident direction of the laser beams to the film was freely chosen. The difference of optical path lengths for three beams from the beam splitters to the film were adjusted by tuning the position of mirrors (mirror1, 2, and 3) within the coherence length of the laser beams (about 10 mm). The positions, and angles of mirror 4,5, and 6 define the lattice symmetry, and the lattice constant of the interference pattern-produced rod-array. For fabrication of a fcc lattice, they were positioned at where the reflected beams produce interference pattern representing periodic rod-array with regular triangle arrangement. The sample stage was tilted so that the interference pattern was inclined by 35° from the vertical. Because of the refractive index difference between air and photoresist film (refractive index of the photoresist before polymerization is 1.67 at 355 nm[11]) laser beams

reflected at the interface. To compensate this effect the tilting angle of the stage was set by 70° . The laser light was exposed by three times while rotating the stage by 120° [12]. A section paper was placed above the sample stage, and the laser beams transmitted through the sample were projected onto the paper. For the alignment of optical path and the position of the sample stage, a spare SU-8 film with a small mark on the rotation center of the stage was prepared. The projection spots of the laser beams on the section paper was monitored with rotating the stage. Position of the sample stage was aligned where the shadow of the mark was always seen on the center of the projection of each laser beam during the rotation, so that the three laser beams intersected each other on the SU-8 film and also on the rotation axis of the stage. The wavevectors of the laser beams were also adjusted from the position of the projection spots on the section paper relative to the distance from the stage to the paper.

The photoresist we used is epoxy resin SU-8 2035(MicroChem Co. Ltd.). SU-8 was spin-coated on a glass substrate (at 3000 rpm for 1 minute) as the thickness of the film was $35\ \mu\text{m}$. Before laser irradiation we performed two-step soft baking on the film at 65°C for 3 minutes and at 95°C for 5 minutes, and left the film in a dark room for several minutes for cooling. After laser irradiation we again performed two-step post expose baking at 65°C for 1 minutes and at 95°C for 3 minutes to cross-link the polymer of exposed parts. 1-methoxy-2-propylacetate was used to develop the fabricated structures. The total intensity of the incident laser beams was $2.5\ \text{mW}/\text{mm}^2$, and the exposure time was $1/60$ second for one irradiation.

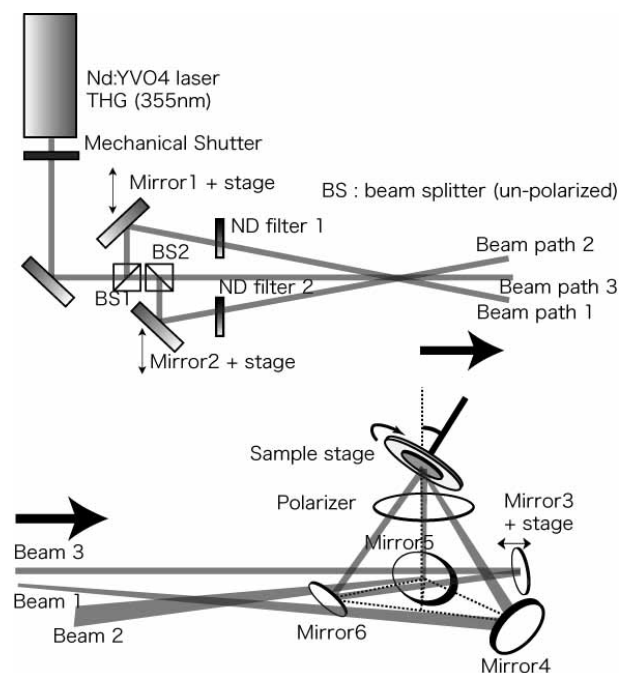


Fig. 3. Optical setup for the three-beam three-times laser interference patterning.

Fig. 4(a) shows an scanning electron microscope (SEM) image of the fabricated structure. The distance of the nearest neighbor rods is $1.0\ \mu\text{m}$, which corresponds to the lattice constant of $1.4\ \mu\text{m}$, and the diameter of the rods is $0.5\ \mu\text{m}$. The whole size of the structure is $1\ \text{mm} \times 1\ \text{mm} \times 30\ \mu\text{m}$, which is corresponding to about $600 \times 600 \times 20$ crystal periods. We observed a lot of cracks in the rim of the structure running straight along crystal axis. Fig. 4(b) and (c) are SEM images of the top surface and the crack of the structure with higher magnifica-

tion. Simulated fcc lattice and its cross section of crystal faces in $\langle 1, 1, 1 \rangle$ and $\langle 1, 1, -1 \rangle$ are shown in Fig. 4(d) and (e). From comparison between SEM images and simulation results, it is seen that cross section images represent the crystal face of $\langle 1, 1, 1 \rangle$ and $\langle 1, 1, -1 \rangle$ respectively. The cracks in the rim of the structure were caused by the shrink of the structure during developing process. From the comparison between the width of the crack and the total size of the structure measured by SEM observation, the shrinkage ratio of the structure is estimated to be about 5%.

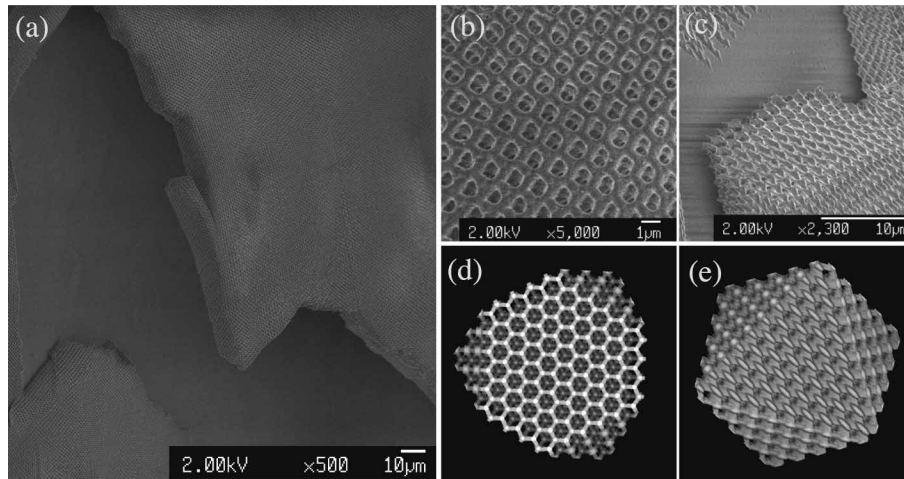


Fig. 4. The scanning electron microscope image of the scaffold type fcc optical lattice. The lattice constant is about $1.5 \mu\text{m}$. (a) A bird's eye view. (b,c) Magnified images of (b) top surface of the structure, and (c) cross section of a crack in the rim of the structure. (d,e) Simulated cross section of fcc lattice in (a) $\langle 1, 1, 1 \rangle$ and (b) $\langle 1, 1, -1 \rangle$.

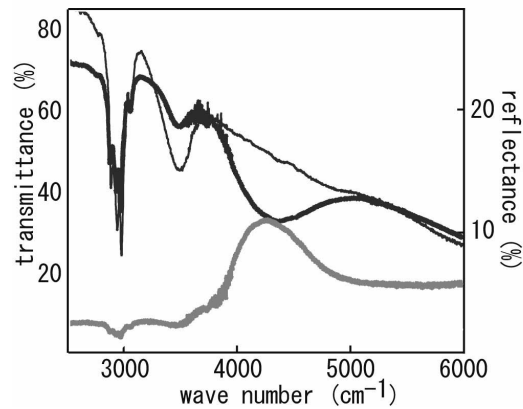


Fig. 5. The transmittance (black thick line) and the reflectance (gray line) spectra of the fabricated structure. The thin black line shows the transmittance spectrum of a SU-8 film as a reference.

We investigated the optical property of the structure by Fourier-transform infrared spectroscopy. A FTIR microscope (Thermo Nicolet co. Ltd., Nexus670 + Nicolet Continuum) with

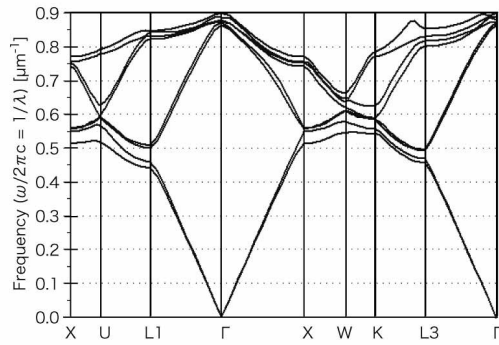


Fig. 6. The photonic band diagram for our fabricated structure. The Brillouin zone of fcc structure and the definition of the symmetry points can be found in ref.12. The gap opens in the $\Gamma - L3$ direction at a frequency of 4500 cm^{-1} .

a Cassegrainian objective lens with $\text{NA}=0.65$ was used to measure transmission, and reflection spectra, and the spectra was measured in the $\langle 1, 1, 1 \rangle$ direction. Fig. 5 shows the spectra, as well as the transmission spectrum of SU-8 polymer film itself. Two depression dips at 3000 cm^{-1} and 3500 cm^{-1} in both of transmittance and reflectance are attributed to the absorption of the SU-8 polymer. We observed another broad dip in transmission and a simultaneous reflection peak at around 4300 cm^{-1} , which corresponds to the wavelength of $2.3 \mu\text{m}$. The lattice periodicity in the $\langle 1, 1, 1 \rangle$ direction in the fabricated structure is about $0.8 \mu\text{m}$. The refractive index of SU-8 is 1.57 at near infrared region. By judging the lattice constant and the diameter of the rods the filling fraction and the mean refractive index of the structure is estimated as 80% and 1.46 , respectively. From these value the wavelength of photonic band gap in the $\langle 1, 1, 1 \rangle$ direction is approximately estimated as $2.33 \mu\text{m}$. We also calculated the photonic band diagram by three-dimensional plane wave approximation method[12] as shown in Fig. 6. In the photonic band diagram the direction of $\Gamma - L3$ is equivalent to the $\langle 1, 1, 1 \rangle$ direction. Since the refractive index of SU-8 polymer is low there is no absolute photonic band gap in the structure, and in the $\Gamma - L3$ direction the gap opens at a frequency of 4500 cm^{-1} . This diagram also shows a good agreement with our experimental results. We concluded that the enhancement of reflection and depression in transmission around 4300 cm^{-1} appeared by Bragg diffraction of light by the lattice structure.

4. Conclusion

In conclusion, we reported three-step three-beam interference exposure and fabrication of scaffold type 3D photonic crystal structures of three intersecting rod arrays. We showed a simple routine to seek the geometrical configuration of the incident beams for all fourteen Bravais lattices, and experimentally demonstrated the principle of the method. It is known that the diamond-like architecture yields the largest 3D photonic band gap. Application of the multi-step multi-beam lasers interference patterning for diamond geometry is the next step of the research.